SISSA

Gamma ray lines from a universal extra dimension

To cite this article: Gianfranco Bertone *et al* JCAP03(2012)020

View the article online for updates and enhancements.

Gamma ray lines from a universal extra dimension

Gianfranco Bertone,[a,b] **C. B. Jackson,**[c] **Gabe Shaughnessy,**[d,e]
Tim M.P. Tait[f] **and Alberto Vallinotto**[g]

[a]Institut for Theoretical Physics, Univ. of Zürich,
 Winterthurerst. 190, 8057 Zürich CH

[b]IAP, UMR 7095-CNRS, Univ. P. et M. Curie,
 98bis Bd Arago, 75014 Paris, France

[c]Department of Physics, University of Texas at Arlington,
 Arlington, TX 76019, U.S.A.

[d]High Energy Physics Division, Argonne National Laboratory,
 Argonne, IL 60439, U.S.A.

[e]Northwestern University, 2145 Sheridan Road,
 Evanston, IL 60208, U.S.A.

[f]Department of Physics and Astronomy, University of California,
 Irvine, CA 92697, U.S.A.

[g]Center for Particle Astrophysics, Fermi National Accelerator Laboratory,
 Batavia, IL 60510, U.S.A.
 E-mail: G.Bertone@uva.nl, cbjackson@uta.edu, gshau@hep.wisc.edu,
 ttait@uci.edu, avallino@gmail.com

Abstract. Indirect Dark Matter searches are based on the observation of secondary particles produced by the annihilation or decay of Dark Matter. Among them, gamma-rays are perhaps the most promising messengers, as they do not suffer deflection or absorption on Galactic scales, so their observation would directly reveal the position and the energy spectrum of the emitting source. Here, we study the detailed gamma-ray energy spectrum of Kaluza-Klein Dark Matter in a theory with 5 Universal Extra Dimensions. We focus in particular on the two body annihilation of Dark Matter particles into a photon and another particle, which produces monochromatic photons, resulting in a line in the energy spectrum of gamma rays. Previous calculations in the context of the five dimensional UED model have computed the line signal from annihilations into $\gamma\gamma$, but we extend these results to include γZ and γH final states. We find that these spectral lines are subdominant compared to the predicted $\gamma\gamma$ signal, but they would be important as follow-up signals in the event of the observation of the $\gamma\gamma$ line, in order to distinguish the 5d UED model from other theoretical scenarios.

Contents

1 Introduction

There is overwhelming evidence that our Universe contains a large component of non-baryonic dark matter. However, so far its identity and nature have remained elusive [1]. Understanding dark matter in a larger context remains one of the most compelling mysteries in particle astrophysics. With the advent of the current generation of gamma ray and neutrino observatories, the next generation of direct detection experiments, and the successful operation of the Large Hadron Collider, we have entered a promising era for the detection of dark matter through non-gravitational interactions with the Standard Model (SM).

One of the deep mysteries of dark matter is the fact that on the one hand it must be massive, but on the other, incredibly stable, with a lifetime on the order of the age of the Universe itself. This odd combination of features argues for the presence of a symmetry which (at least to very good approximation) forbids the dark matter from decaying. The most straight-forward realization is a symmetry requiring dark matter to couple in pairs with the Standard Model and we can classify theories of dark matter based on how they realize this symmetry.

The most well known example of such a symmetry is the R-parity often built into supersymmetric extensions of the SM to forbid dangerous interactions leading to large baryon- and lepton-number violation. While the fact that R-parity leads naturally to a weakly interacting massive particle (WIMP) that can play the role of dark matter makes it a very attractive ingredient, the existence of R-parity itself is somewhat ad hoc. It would be preferable to have a symmetry whose origin has a deeper motivation.

A wide class of theories with extra dimensions naturally have such a symmetry. The existence of extra dimensions leads to additional spacetime symmetries, some remnant of which may survive compactification of the extra dimensions. In Universal Extra Dimensions (UED), the entire Standard Model lives equally in all dimensions. As a result, there is naively a translational invariance along the extra dimensional directions which translates into conservation of Kaluza Klein (KK) number in the interactions of the modes [2]. In practice, the need for chiral fermions in the low energy theory selects orbifold compactifications which break the conservation of KK number into a Z_2 symmetry, but this is sufficient to guarantee a stable particle which can play the role of dark matter.

The simplest example of UED is a model with five dimensions (5d), four of which are ordinary spacetime with the remaining one compactified into a line segment of length L. The lightest Kaluza Klein (KK) mode is stable, and provided it is weakly interacting, can take the role of dark matter in the Universe. A standard thermal history of the Universe results in the correct relic density for masses on the order of several hundred GeV [3, 4], a region which is also consistent with Tevatron and precision electroweak bounds [5, 6] and a discovery of at least part of the first level of KK modes at the LHC [6, 7]. There are also prospects for direct [8, 9] and indirect [10–14] detection by experiments in the near future.

In this article, we focus in particular on the prospects for detecting gamma rays from annihilation of WIMPs in the galactic halo. Gamma rays offer a particularly promising avenue to detect WIMP annihilations, because they point back to their sources, unlike charged particles, which are at the mercy of the galactic magnetic fields. However, the backgrounds from gamma ray sources are not very well understood, particularly around the galactic center where the concentration of WIMPs is greatest. Thus, we focus on the particular signal of a two body annihilation of two WIMPs into a photon and another particle, which produces monochromatic photons, resulting in a "line" in the energy spectrum of gamma rays. This feature is sufficiently distinct from anything produced by conventional astrophysics so as to perhaps balance the smaller rate caused by the fact that it is a loop-induced process [15]. The Fermi gamma ray observatory is actively searching for such lines as an unequivocal signal of dark matter [16], and predictions from a wide variety of particle physics models have appeared in the literature [17–21].

Previous calculations in the context of the five dimensional UED model have computed the line signal from WIMPs annihilating into $\gamma\gamma$ [14]. We extend these results to include γZ and γH final states (and we independently verify the results of [14], finding agreement for the $\gamma\gamma$ channel). While both γZ and γH turn out to be subdominant compared to the predicted $\gamma\gamma$ signal, they would be important as follow-up signals in the event of the observation of the $\gamma\gamma$ line, in order to distinguish the 5d UED model from other possibilities. For example, the relative strengths of the $\gamma\gamma$ and γZ lines encodes the fact that the LKP couples proportionally to hypercharge, and the existence of a γH line, in addition to being interesting in its own right, is only expected to be visible for a WIMP which is a vector (such as the LKP) or a Dirac fermion.

We proceed as follows. In section 2, we briefly review the 5 dimensional UED model, and the couplings necessary for our later computations. Sections 3 and 4 respectively cover the expected gamma ray continuum and lines resulting from LKP annihilations. Astrophysical inputs, the effects of finite detector energy resolution, and the gamma ray spectra are assembled in section 5. We conclude in section 6.

2   5d UED model

The 5d UED model [2] consists of the ordinary four large space + time dimensions, with one additional spatial dimension compactified into a line segment of length L. Generic points in five dimensional space can be written $x^M \equiv (x^\mu, y)$, where x^μ is the subspace of the four large spacetime dimensions and $0 \leq y \leq L$ is the compact dimension. The Standard Model field content is promoted to functions of the complete spacetime x^M, with the zero modes in the Kaluza-Klein expansion identified with the familiar SM fields. In the discussion below, we will interchangeably refer to the ordinary SM fields as either "SM fields" or "zero-modes".

After electroweak symmetry-breaking, the lightest states obtain the usual SM masses, but we nonetheless continue to refer to them as zero modes in the Kaluza-Klein sense.

Orbifold boundary conditions project out the zero modes of the fifth components of the gauge fields (the higher components are eaten by the KK gauge bosons as per the usual extra-dimensional Higgs mechanism) and the unwanted zero mode degrees of freedom of the fermions. The boundary conditions lead inevitably [22] to the presence of brane-localized terms which further shift the masses of the higher KK modes and break translational invariance along the extra dimension into a discrete parity under which the odd-numbered KK modes are odd and the even-numbered modes are even [23, 24]. As a consequence of this Z_2 remnant symmetry, the lightest first level Kaluza-Klein particle (LKP) is stable.

We follow the general picture of "minimal UED" (mUED) [6, 23] in which the brane terms take sizes which are dictated by loops of bulk couplings, but we do not strictly restrict ourselves to the masses and couplings of mUED.[1] Consequently, the mass spectrum is chiefly characterized by the KK number n, with the masses of all of the particles at that level given roughly by

$$M_n \simeq \frac{\pi n}{L}. \tag{2.1}$$

The boundary terms lead to corrections for the various particles within a given level. mUED predicts the colored particles receive the largest positive corrections to their masses, followed by the SU(2)-charged states. The lightest KK modes of a given level are typically the KK modes of the right-handed charged leptons and the U(1) gauge boson itself. The LKP is thus the first level KK mode of B_μ, and represents a vector dark matter particle (often refered to as the "KK photon") which is a SM gauge singlet. Its principle interactions are to a first level KK fermion and its corresponding zero mode, proportional to the hypercharge of the fermion in question and the gauge coupling g_Y.

The primary couplings of interest here are the couplings of the LKP to one KK fermion and one zero mode fermion, and the couplings of ordinary photons, Z bosons, and Higgs bosons to either zero mode or KK fermions. The photon couples to a pair of either SM or KK fermions proportional to eQ where Q is the electric charge as usual. The SM Higgs couples to a pair of zero modes proportionally to their mass, or to a pair of KK fermions (one of which must be an SU(2) doublet and the other an SU(2) singlet) proportionally to the mass of the analogue zero mode fermion.

The SM Z boson has the standard chiral couplings to the SM fermions, and vector-like couplings to singlet (s) and doublet (d) KK fermions given by:

$$-\frac{e}{4s_w c_w} (g_V + g_A) Z_\mu \bar{\xi}_s^{(1)} \gamma^\mu \xi_s^{(1)} \tag{2.2}$$

and:

$$-\frac{e}{4s_w c_w} (g_V - g_A) Z_\mu \bar{\xi}_d^{(1)} \gamma^\mu \xi_d^{(1)} \tag{2.3}$$

where $\xi_d^{(1)}$ is the first level KK mode of a SM SU(2) doublet, and $\xi_s^{(1)}$ is the first level KK mode of a SM singlet. $s_w(c_w)$ are the sine (cosine) of the weak mixing angle and g_V and g_A are defined as:

$$g_V = -2T_3 + 4Q_f s_w^2 \tag{2.4}$$

$$g_A = 2T_3. \tag{2.5}$$

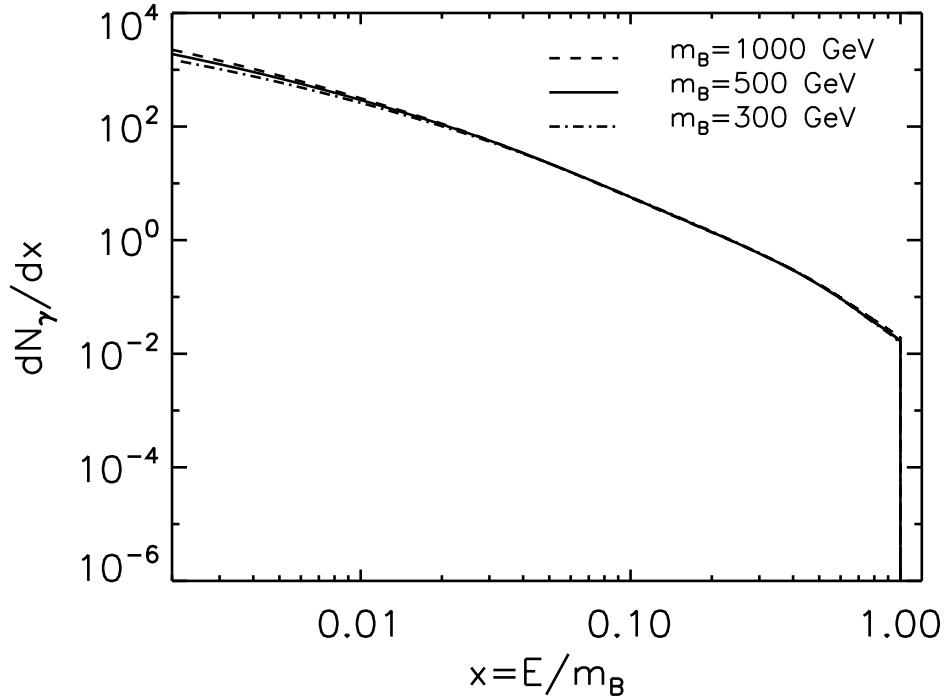[1]For a few interesting examples of more severe deviations from mUED, see refs. [25].

Figure 1. The continuum gamma ray spectrum as a function of x, the ratio of the photon energy to the LKP mass, for LKP masses $m_B = 300\,\mathrm{GeV}$ (dash-dotted curve), $500\,\mathrm{GeV}$ (dashed curve), and $1\,\mathrm{TeV}$ (solid curve).

The $B^{(1)}$ couples to one SM fermion and one KK fermion as:

$$- g_Y \frac{Y_s}{2} B_\mu^{(1)} \bar{\xi}_s^{(1)} \gamma^\mu \left(1 + \gamma_5\right) \psi^{(0)} + c.c. \tag{2.6}$$

and:

$$- g_Y \frac{Y_d}{2} B_\mu^{(1)} \bar{\xi}_d^{(1)} \gamma^\mu \left(1 - \gamma_5\right) \psi^{(0)} + c.c.. \tag{2.7}$$

where $\psi^{(0)}$ is the zero mode fermion.

3 Continuum gamma rays

Annihilations of two LKPs is predominantly into charged leptons ($\sim 59\%$), with significant fractions into quarks ($\sim 35\%$), neutrinos ($\sim 4\%$), and Higgs bosons ($\sim 2\%$) [3]. The fact that a large fraction of annihilations produces hard charged leptons has the consequence that the continuum gamma ray signal is itself rather hard [8, 13], which distinguishes the 5d continuum spectrum from the six dimensional chiral square model [17]. The resulting continuum spectrum is shown in figure 1 as a function of $x \equiv E_\gamma / M_B$, the fraction of energy of the final state photon normalized to the LKP mass. Comparing curves for LKP masses of 300, 500, and 1000 TeV, we see little difference in the photon spectrum, which is easily explained by the fact that the annihilations are almost entirely into light SM particles.
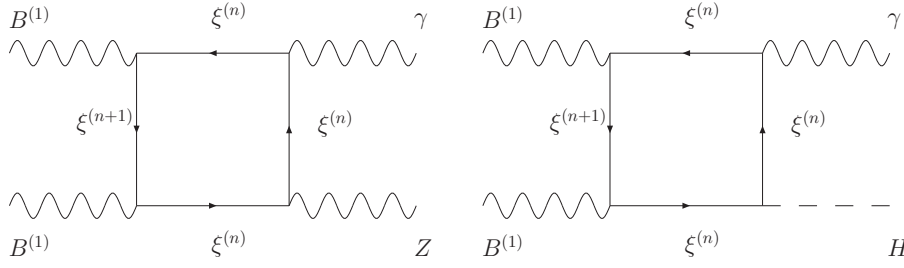
Figure 2. Examples of Feynman diagrams which contribute to (a) $B^{(1)}B^{(1)} \to \gamma + Z$ and (b) $B^{(1)}B^{(1)} \to \gamma + H$.

4 Gamma ray line cross sections

In addition to a diffuse continuum of gamma rays, WIMP annihilations are also expected to produce prompt photons via loop-level processes. These types of annihilations produce $\gamma + X$ final states (where X can be either a vector gauge boson or a scalar) and result in mono-energetic "lines" superimposed on the continuum. The energy of these lines are determined almost solely by the mass of the WIMP and the X particle:

$$E_\gamma = M_{WIMP}\left(1 - \frac{M_X^2}{4M_{WIMP}^2}\right).\tag{4.1}$$

Due to the non-relativistic nature of WIMPs, the possible final states (i.e., the identity of X) are determined by the spin of the DM particle. In the case of the 5d UED model, the WIMP is a vector gauge boson and, hence, X can be either a vector or a scalar. In other words, WIMP annihilations in the 5d UED model are capable of producing $\gamma\gamma$, γZ and (if kinematically-accessible) γH final states (where H is the SM Higgs boson).

The production of the $\gamma\gamma$ final state in the 5d UED model was first considered in ref. [14]. Here, we will focus on the other two possible final states (γZ and γH) and we refer the interested reader to the above reference for details on the calculation of the $\gamma\gamma$ cross section. We have verified the results from the previous analysis and we present the numerical results for the flux in the following sections.

Representative Feynman diagrams depicting the process $B^{(1)} + B^{(1)} \to \gamma + X$ (where $X = Z$ or H) are shown in figure 2. Note that since the LKP is to very good approximation pure $B^{(1)}$ ($\lesssim 10^{-1}$ for mUED boundary terms and $L^{-1} \gtrsim 300\,\text{GeV}$ [23]), loops containing W and/or KK charged Goldstone bosons are suppressed by the tiny $W_3^{(1)}$ content. We neglect these tiny contributions compared to the dominant diagrams consisting of closed loops of SM and KK fermions.

4.1 Annihilation to $\gamma + Z$

For the $\gamma + Z$ process, we assign Lorentz indices and momenta as

$$B_{\mu_1}^{(1)}(p_1) + B_{\mu_2}^{(1)}(p_2) \to \gamma_{\mu_3}(p_3) + Z_{\mu_4}(p_4).\tag{4.2}$$

Following ref. [14], the scattering amplitude involving four external gauge bosons can be written as:

$$\mathcal{M} = \epsilon_1^{\mu_1}(p_1)\epsilon_2^{\mu_2}(p_2)\epsilon_3^{\mu_3*}(p_3)\epsilon_4^{\mu_4*}(p_4)\mathcal{M}_{\mu_1\mu_2\mu_3\mu_4}(p_1,p_2,p_3,p_4).\tag{4.3}$$

In general, the subamplitude $\mathcal{M}_{\mu_1\mu_2\mu_3\mu_4}$ can be expanded in terms of metric tensors and external momenta. Taking into account the transversality of the polarization tensors ($\epsilon(p) \cdot p = 0$) and the non-relativistic nature of WIMPs today (such that $p_1 \simeq p_2 \equiv p$), the most general form is given by:

$$
\begin{aligned}
\mathcal{M}^{\mu_1\mu_2\mu_3\mu_4} &= \frac{\alpha_Y \alpha_{em}}{4c_w s_w} \sum_\ell Q_\ell \bigg[\frac{A_\ell}{m_{B^{(1)}}^4} p_3^{\mu_1} p_4^{\mu_2} p^{\mu_3} p^{\mu_4} + \frac{B_{\ell,1}}{m_{B^{(1)}}^2} g^{\mu_1\mu_2} p^{\mu_3} p^{\mu_4} + \frac{B_{\ell,2}}{m_{B^{(1)}}^2} g^{\mu_1\mu_3} p_4^{\mu_2} p^{\mu_4} \\
&\quad \frac{B_{\ell,3}}{m_{B^{(1)}}^2} g^{\mu_1\mu_4} p_4^{\mu_2} p^{\mu_3} + \frac{B_{\ell,4}}{m_{B^{(1)}}^2} g^{\mu_2\mu_3} p_3^{\mu_1} p^{\mu_4} + \frac{B_{\ell,5}}{m_{B^{(1)}}^2} g^{\mu_2\mu_4} p_3^{\mu_1} p^{\mu_3} \\
&\quad + \frac{B_{\ell,6}}{m_{B^{(1)}}^2} g^{\mu_3\mu_4} p_3^{\mu_1} p_4^{\mu_2} + C_{\ell,1} g^{\mu_1\mu_2} g^{\mu_3\mu_4} + C_{\ell,2} g^{\mu_1\mu_3} g^{\mu_2\mu_4} + C_{\ell,3} g^{\mu_1\mu_4} g^{\mu_2\mu_3} \bigg] \\
&\equiv \frac{\alpha_Y \alpha_{em}}{4c_w s_w} \sum_\ell Q_\ell \mathcal{A}_{ZA,\ell}^{\mu_1\mu_2\mu_3\mu_4} .
\end{aligned}
\tag{4.4}
$$

where we have pulled out a common factor with $\alpha_Y = \alpha_{em}/c_w^2$ and we sum over all charged fermions running in the loop. The fact that the WIMPs are annihilating nearly at rest (i.e., $p^\mu \simeq (m_{B^{(1)}}, \mathbf{0})$) also allows one to define the z-axis in the center-of-mass frame as the axis along which the final state particles are traveling. This simplifies things greatly as many of the dot products between polarization tensors and momentum vectors vanish. Accounting for this and imposing conservation of momentum ($2p = p_3 + p_4$), we find that the only remaining tensor structures are B_2, B_4, B_6, C_1, C_2 and C_3.

Computation of the loop integrals in WIMP annihilations is complicated by the fact that two of the incoming momenta are nearly identical. In these configurations, usual approaches such as the Passarino-Veltman scheme [26] for computing tensor integrals break down and one must rely on alternative schemes in order to safely compute one-loop scattering amplitudes. We have chosen to use the scheme introduced in ref. [27]. This scheme was most recently used to compute one-loop WIMP annihilation scattering amplitudes and we refer the interested reader to in ref. [17] for details.

Squaring the amplitude and summing/averaging over all polarizations, we find that the cross section for $B^{(1)} + B^{(1)} \rightarrow \gamma + Z$ takes the form:

$$
\langle \sigma_{\gamma Z} v \rangle = \frac{1}{9} \frac{\alpha_Y^2 \alpha_{em}^2}{16\pi c_w^2 s_w^2} \left(\frac{\beta_Z^2}{32 m_{B^{(1)}}^2} \right) \left| \sum_\ell Q_\ell \mathcal{A}_{ZA,\ell} \right|^2 ,
\tag{4.5}
$$

where $\beta_Z = \sqrt{1 - \frac{m_Z^2}{4 m_{B^{(1)}}^2}}$.

4.2 Annihilation to $\gamma + H$

The amplitude for this process takes the form:

$$
\mathcal{M} = \epsilon_1^{\mu_1}(p_1) \epsilon_2^{\mu_2}(p_2) \epsilon_3^{\mu_3*}(p_3) \mathcal{M}_{\mu_1\mu_2\mu_3}(p_1, p_2, p_3, p_4)
\tag{4.6}
$$

where we have assigned the Lorentz indices and momenta as

$$
B_{\mu_1}^{(1)}(p_1) + B_{\mu_2}^{(1)}(p_2) \rightarrow \gamma_{\mu_3}(p_3) + H(p_4).
\tag{4.7}
$$

The amplitudes for this process involve one less vector boson, and thus have a simpler tensor structure than the γZ case. In fact, due to the scalar coupling of the Higgs boson, the only

surviving terms from the trace over the internal fermion line are proportional to Levi-Civita tensors $\epsilon^{\mu\nu\lambda\sigma}$ contracted with at least one of the external momenta. Instead of expanding the scattering amplitude in terms of all possible permutations, we only list the surviving terms once the non-relativistic nature of the WIMPs and conservation of momentum are applied. The resulting expression takes the form:

$$
\begin{aligned}
\mathcal{M}_{\mu_1\mu_2\mu_3}(p_1, p_2, p_3, p_4) &= \frac{\alpha_Y \alpha_{em}}{2 m_W s_w} \sum_{\ell} Q_\ell m_\ell \left(Y_{\ell,d}^2 - Y_{\ell,s}^2 \right) \left[\frac{D_1}{m_{B^{(1)}}^3} p_A^{\mu_1} p_\sigma p_{A,\lambda} \epsilon^{\sigma\lambda\mu_2\mu_3} \right. \\
&\quad \left. + \frac{D_2}{m_{B^{(1)}}} p_\sigma \epsilon^{\sigma\mu_1\mu_2\mu_3} + \frac{D_3}{m_{B^{(1)}}} p_{A,\sigma} \epsilon^{\sigma\mu_1\mu_2\mu_3} \right] \\
&\equiv \frac{\alpha_Y \alpha_{em}}{2 m_W s_w} \sum_{\ell} Q_\ell m_\ell \left(Y_{\ell,d}^2 - Y_{\ell,s}^2 \right) \mathcal{A}_{HA,\ell}^{\mu_1\mu_2\mu_3} .
\end{aligned}
\tag{4.8}
$$

We note that the scattering amplitude is directly proportional to the zero mode fermion mass m_ℓ (via the Yukawa coupling). As a result, only loops containing top quarks and their KK partners will make a significant contribution to the process. Summing and averaging over all polarizations, we find the cross section can be written as:

$$
\langle \sigma_{\gamma H} v \rangle = \frac{1}{9} \frac{\alpha_Y^2 \alpha_{em}^2}{4\pi m_W^2 s_w^2} \left(\frac{\beta_H^2}{32 m_{B^{(1)}}^2} \right) \left| \sum_{\ell} Q_\ell m_\ell \left(Y_{\ell,d}^2 - Y_{\ell,s}^2 \right) \mathcal{A}_{HA,\ell} \right|^2 ,
\tag{4.9}
$$

where $\beta_H = \sqrt{1 - \frac{m_H^2}{4 m_{B^{(1)}}^2}}$.

In figure 3, we plot the cross sections for the $\gamma\gamma$, γZ and γH final states as a function of the WIMP mass $m_{B^{(1)}}$ where we have assumed a universal KK fermion mass of $m_\xi \simeq 1.1 \times m_{B^{(1)}}$. From this figure, we see that the γZ cross section is roughly 10% of the $\gamma\gamma$ cross section and is in agreement with the estimation of ref. [14] while the γH cross section is even more suppressed.

5   Gamma ray flux and energy spectrum

The differential flux of photons predicted to be observed at an angle ψ from the direction to the galactic center (GC) is

$$
\frac{d\Phi_\gamma}{d\Omega dE}(\psi, E) = \frac{r_\odot \rho_\odot^2}{4\pi m_{B^{(1)}}^2} \frac{dN_\gamma}{dE} \int_{\text{l.o.s.}} \frac{ds}{r_\odot} \left[\frac{\rho[r(s,\psi)]}{\rho_\odot} \right]^2
\tag{5.1}
$$

with

$$
\frac{dN_\gamma}{dE} = \sum_f \langle \sigma v \rangle_f \frac{dN_\gamma^f}{dE},
\tag{5.2}
$$

where the index f denotes the annihilation channels with one or more photons in the final state, $\langle \sigma v \rangle_f$ is the corresponding cross-section and dN_γ^f/dE is the (normalized) photon spectrum per annihilation. Furthermore, $\rho(\vec{x})$, $\rho_\odot = 0.3 \, \text{GeV/cm}^3$ and $r_\odot = 8.5$ kpc respectively denote the dark matter density at a generic location $\vec{x}$ *with respect to the GC*, its value at the solar system location and the distance of the Sun from the GC. Finally, the coordinate s runs along the line of sight, which in turn makes an angle ψ with respect to the direction of the GC.
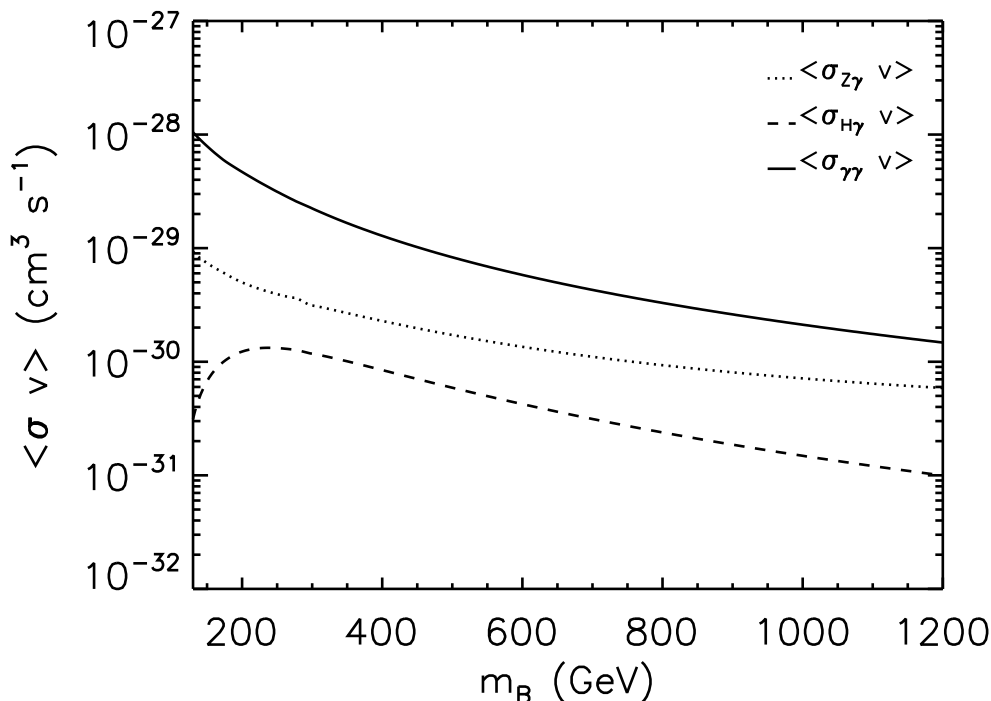
Figure 3. The annihilation cross sections for the $\gamma\gamma$, γZ and γH final states.

Equation (5.1) allows one to separate the factors contributing to the predicted incoming gamma ray flux. In particular, while the dN_γ/dE term is sensitive only to the particle physics under consideration, the remaining factors are sensitive to the modeling of the halo density profile $\rho(\vec{x})$. For a given dark matter model, these latter factors are the main source of uncertainty in the prediction of the detectability of a dark matter signal. To proceed further, we define with J the dimensionless integral along the line-of- sight appearing in eq. (5.1) and with $\bar{J}$ its average value computed for a solid angle $\Delta\Omega$ centered on the GC

$$J \equiv \int_{\text{l.o.s.}} \frac{ds}{r_\odot} \left[\frac{\rho[r(s,\psi)]}{\rho_\odot} \right]^2,$$
$$\bar{J}(\Delta\Omega) = \frac{1}{\Delta\Omega} \int_{\Delta\Omega} J(\psi)\, d\Omega. \tag{5.3}$$

The $\bar{J}$ factor thus defines the normalization of the gamma ray flux signal and allows one to quantify the impact of astrophysical uncertainties due to the lack of knowledge of the halo density profile. In what follows we will consider two models for ρ: the Navarro Frenk and White (NFW) profile and the "adiabatically contracted" profile.

The Navarro Frenk and White (NFW) profile has been shown to fit reasonably well the results from recent high-resolution numerical simulations. This density profile is often used as a benchmark for indirect dark matter searches [28],

$$\rho_{\text{NFW}}(r) = \frac{\rho_s}{\frac{r}{r_s} \left(1 + \frac{r}{r_s}\right)^2}. \tag{5.4}$$

Modifications of the above profile on very small scales have been observed in the most recent simulations. While ref. [29] shows that the innermost regions of DM halos are better

Model	$\bar{J}\left(10^{-5}\right)$
NFW	1.5×10^4
Adiabatic	4.7×10^7

Table 1. Value of $\bar{J}(10^{-5})$ for two dark matter density profiles.

approximated with $r^{-1.2}$ cusps, ref. [30] points out that the analytic form that provides an optimal fit to the simulated halos is the so-called "Einasto profile" [31],

$$\rho(r) = \rho_0 \, \exp\left[-\frac{2}{\alpha}\left(\left(\frac{r}{R}\right)^\alpha - 1\right)\right], \tag{5.5}$$

which is shallower than NFW at very small radii.[2]

The above results have been derived in the framework of simulations containing only dark matter particles, which interact gravitationally. Baryons however are expected to have a non-negligible effect on the small scale dynamics of galaxies. In particular, due to the dissipative nature of the baryonic fluid, when baryons lose energy and contract, this affects the gravitational potential experienced by the dark matter. In the "adiabatic compression" scenario [32], the baryons contraction is quasi-stationary and spherically symmetric. Starting from an initial NFW profile, the final slope in the innermost regions becomes $r^{-1.5}$ [33–36].

Assuming $\Delta\Omega = 10^{-5}$ sr. (corresponding to the angular resolution of the HESS and Fermi LAT γ-ray experiments), in table 1 we show the value of $\bar{J}$ obtained for two profiles: the benchmark NFW profile and the "adiabatically contracted" profile, with the same parameters as the profile labelled 'A' in ref. [36].[3] Table 1 explicitly shows the extent to which the present uncertainty in the knowledge of the halo density profile turns into uncertainty in the predicted gamma ray flux from the GC.

Recently, a large suite of cosmological simulations aimed to study the assembly of Milky Way like galaxies were carried out using the Adaptive Mesh Refinement (AMR) code RAMSES, which includes treatment of dark matter, gas and stars [37] . The modeling included realistic recipes for star formation, supernova feedback (SNII and SNIa), stellar mass loss, gas cooling/heating and metal enrichment. It was found that adopting different prescriptions for the star formation history results in a strong difference not only in galactic disk size and concentration, but also on DM contraction, therefore dramatically affecting the DM profile in the innermost regions of galactic halos.

These simulations were shown to bracket the so-called Kennicutt-Schmidt relation (that parametrizes the star formation rate as a function of the gas density) from the THINGS survey [38] , and they are therefore representative of Milky Way-like galaxies in the local Universe. A comparison of the profiles obtained in these simulations with the standard DM-only case can be found e.g. in ref. [39], where it is also shown that the final profile is substantially different with respect to a naïve implementation of adiabatic contraction. We also stress that DM halos in numerical simulations deviate rather strongly from spherical symmetry, a circumstance that introduces additional uncertainties on the estimate of the integral along the line of sight J [39].

---

[2]The values assumed for the parameters are in this case $\alpha = 0.17$ and $R = 20$ kpc.

[3]Note that our values of J for the NFW and "Adiabatic" profiles are slightly different from the values in ref. [36], due to the fact that the NFW profile was there approximated as a simple r^{-1} power-law from the galactic center to the location of the Sun.

Other processes due to the gravitational interaction of baryons (such as the "heating" of the DM fluid) can possibly have the opposite effect on the final DM distribution and soften the central cusps. Furthermore, the presence of a super-massive black hole (BH) at the GC inevitably affects the DM profile. The growth of the BH from an initial small seed would initially lead to a large DM "spike" [40]. While dynamical effects and DM annihilations will subsequently tend to destroy the spike [36, 41, 42], in some cases significant overdensities can survive over a Hubble time.

In what follows, the predicted gamma ray flux from the galactic center is obtained assuming the NFW halo profile. To obtain predictions for other profiles, it is sufficient to rescale the flux by the appropriate ratio of $\bar{J}$ (which is $3.3 \cdot 10^3$ for a naïve implementation of adiabatic contraction).

Finally, we account for the finite resolution of the detector by convolving the unfiltered signal $S(E)$ with a gaussian kernel $G(E, E_0)$,

$$G(E, E_0) = \frac{1}{\sqrt{2\pi}E_0\sigma} \exp\left[-\frac{(E - E_0)^2}{2\sigma^2 E_0^2}\right], \tag{5.6}$$

where σ is related to the detector's relative energy resolution ξ by $\sigma = \xi/2.3$. The signal $S_M(E_0)$ measured by the detector at energy E_0 is then simply given by

$$S_M(E_0) = \int dE\, G(E, E_0)\, S(E). \tag{5.7}$$

Combining the expectations for $\bar{J}$ with the particle physics rates and the detector response, we arrive at predictions for the flux and spectrum of gamma rays. In figures 4, 5 and 6, we show predictions for the flux for an NFW halo profile and three choices of LKP mass. Although the thermal relic density favors LKPs in the range of 500–900 GeV [3, 4], we consider a wider range of LKP masses motivated by the possibility that the LKP is not a canonical thermal relic, which could allow for a wider range of masses consistent with the observed quantity of dark matter in the Universe. For example, if the modulus which controls the size of the extra dimension is cosmologically active, it could cause large deviations in the thermodynamics of the Universe from its extrapolated history [43]. Alternately, early production of KK gravitons which eventually decay into LKPs can serve as a nonthermal production mechanism for KK dark matter in an otherwise standard cosmological history [44].

Figures 4–6 contain curves for three different choices of energy resolutions, ranging from the $\sim 10\%$ resolution typical of current experiments, to an aggressive 0.5% resolution which might be possible in future experiments. We find that at 10% energy resolution, lines in the 5d UED model are very difficult to distinguish from the continuum. At a 5% energy resolution, broad lines may appear for LKP masses around 300 GeV, slightly above the lower bound from colliders. At 0.5%, well separated lines for $\gamma\gamma$, γZ, and γH are visible for light LKPs, and some structure related to the γH line is visible for an LKP mass of around 500 GeV.

In principle, we should compare our predicted flux with gamma ray observations, since data are available from a variety of gamma-ray telescopes, such as the Fermi LAT and Air Cherenkov Telescopes like HESS and MAGIC. The comparison is however made complicated by the aforementioned uncertainties on the normalization of the predicted flux on one side, and on the other by the difficult interpretation of astrophysical data.

It is for instance unclear at this stage whether known astrophysical sources can account for the energy spectrum obtained by Fermi. A recent analysis of a $1° \times 1°$ found that the
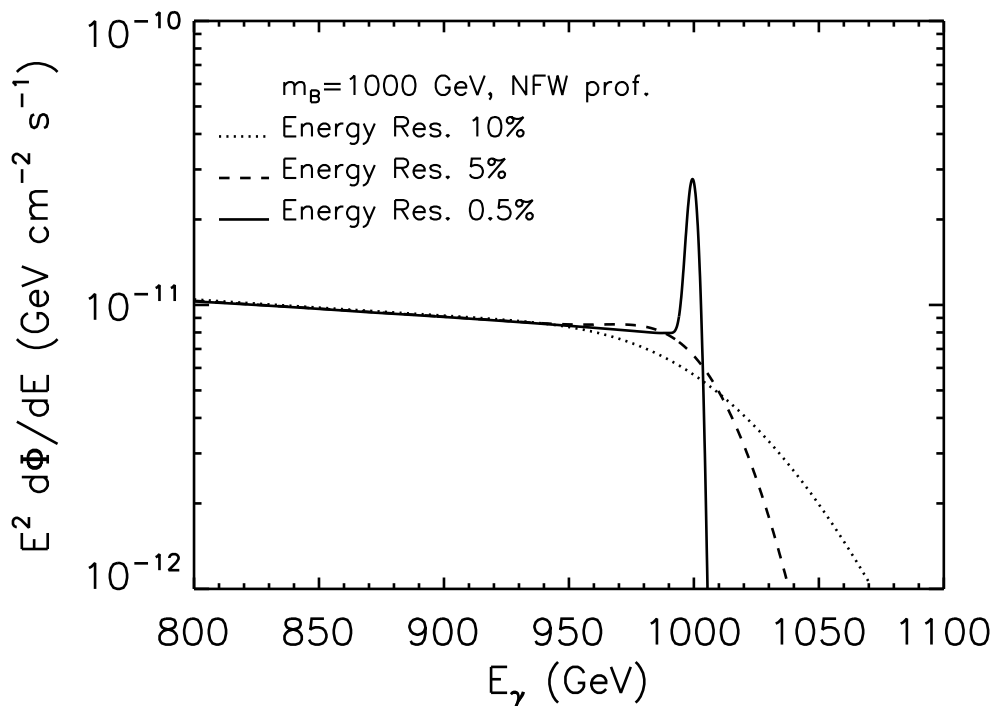
Figure 4. The gamma ray flux as a function of the photon's energy for a WIMP of mass 1 TeV. Shown are three different experimental energy resolutions.
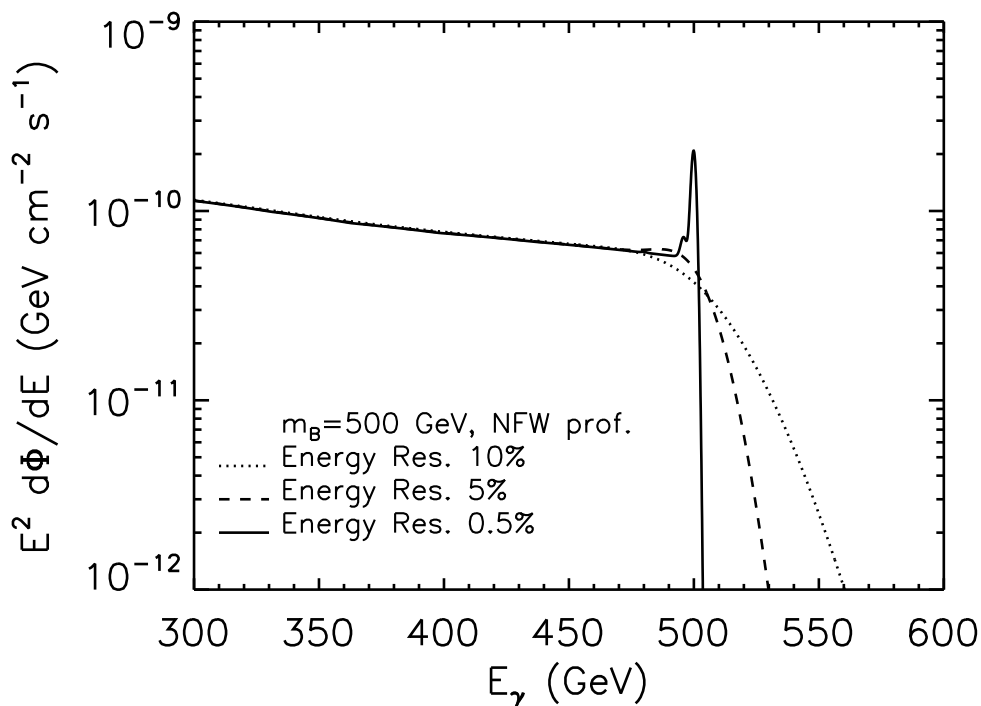

Figure 5. The gamma ray flux as a function of the photon's energy for a WIMP of mass 500 GeV. Shown are three different experimental energy resolutions.
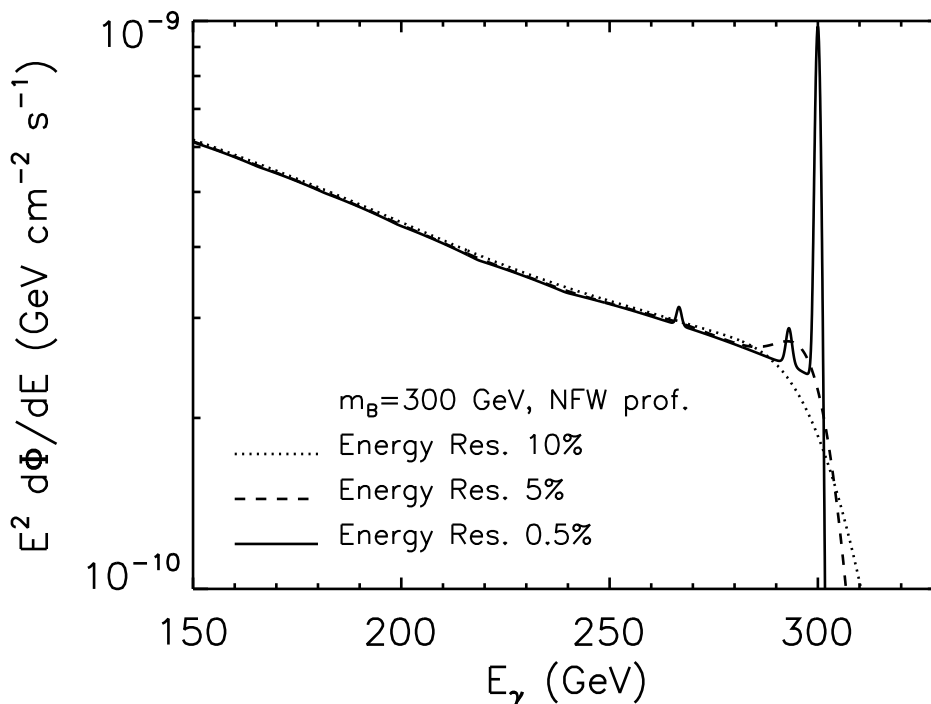
Figure 6. The gamma ray flux as a function of the photon's energy for a WIMP of mass 300 GeV. Shown are three different experimental energy resolutions.

diffuse gamma-ray background and discrete sources, as estimated with standard astrophysical tools, can account for practically all the observed flux, but there is a small excess at energies $\mathcal{O}(1)$ GeV, which may or may not be explained with an improved model of the Galactic diffuse emission and with a better understanding of the systematic errors [45]. At the same time, there is an ongoing debate on the possible origin of the point source observed by HESS right at the Galactic center [46].

In principle, once these issues are settled, and the astrophysical backgrounds are well-known, one can search for a DM signal even in the case where it provides a subdominant contribution to the total flux. More subtle features such as subdominant gamma-ray lines could therefore in principle emerge in the process of data analysis, in which case one could try to perform the program describe above, and search for additional lines that might shed light on the structure of the dark sector.

6 Conclusions

Extra dimensions are a fascinating possibility in the spectrum of physics beyond the Standard Model, one which leads to a unique mechanism to provide a stable WIMP to play the role of dark matter. We have examined the gamma ray line signals for UED dark matter WIMPs, extending the results for $\gamma\gamma$ in the literature [14] to also include lines from γZ and γH final states. Our conclusions are that such lines are very challenging for the current generation of gamma ray observatories to resolve, but may be visible at the next generation of such experiments. As such experiments are designed, we hope our work will be of some value in evaluating their exciting physics capabilities.

Acknowledgments

References

[1] G. Bertone, D. Hooper and J. Silk, *Particle dark matter: Evidence, candidates and constraints*, *Phys. Rept.* **405** (2005) 279 [`hep-ph/0404175`] [INSPIRE].

[2] T. Appelquist, H.-C. Cheng and B.A. Dobrescu, *Bounds on universal extra dimensions*, *Phys. Rev.* **D 64** (2001) 035002 [`hep-ph/0012100`] [INSPIRE].

[3] G. Servant and T.M.P. Tait, *Is the lightest Kaluza-Klein particle a viable dark matter candidate?*, *Nucl. Phys.* **B 650** (2003) 391 [`hep-ph/0206071`] [INSPIRE].

[4] K. Kong and K.T. Matchev, *Precise calculation of the relic density of Kaluza-Klein dark matter in universal extra dimensions*, *JHEP* **01** (2006) 038 [`hep-ph/0509119`] [INSPIRE];
F. Burnell and G.D. Kribs, *The Abundance of Kaluza-Klein dark matter with coannihilation*, *Phys. Rev.* **D 73** (2006) 015001 [`hep-ph/0509118`] [INSPIRE];
M. Kakizaki, S. Matsumoto, Y. Sato and M. Senami, *Relic abundance of LKP dark matter in UED model including effects of second KK resonances*, *Nucl. Phys.* **B 735** (2006) 84 [`hep-ph/0508283`] [INSPIRE];
M. Kakizaki, S. Matsumoto and M. Senami, *Relic abundance of dark matter in the minimal universal extra dimension model*, *Phys. Rev.* **D 74** (2006) 023504 [`hep-ph/0605280`] [INSPIRE];
S. Matsumoto, J. Sato, M. Senami and M. Yamanaka, *Relic abundance of dark matter in universal extra dimension models with right-handed neutrinos*, *Phys. Rev.* **D 76** (2007) 043528 [`arXiv:0705.0934`] [INSPIRE].

[5] T. Appelquist and H.-U. Yee, *Universal extra dimensions and the Higgs boson mass*, *Phys. Rev.* **D 67** (2003) 055002 [`hep-ph/0211023`] [INSPIRE];
T. Flacke, D. Hooper and J. March-Russell, *Improved bounds on universal extra dimensions and consequences for LKP dark matter*, *Phys. Rev.* **D 73** (2006) 095002 [*Erratum ibid.* **D 74** (2006) 019902] [`hep-ph/0509352`] [INSPIRE];
I. Gogoladze and C. Macesanu, *Precision electroweak constraints on Universal Extra Dimensions revisited*, *Phys. Rev.* **D 74** (2006) 093012 [`hep-ph/0605207`] [INSPIRE].

[6] H.-C. Cheng, K.T. Matchev and M. Schmaltz, *Bosonic supersymmetry? Getting fooled at the CERN LHC*, *Phys. Rev.* **D 66** (2002) 056006 [`hep-ph/0205314`] [INSPIRE].

[7] A. Datta, K. Kong and K.T. Matchev, *Discrimination of supersymmetry and universal extra dimensions at hadron colliders*, *Phys. Rev.* **D 72** (2005) 096006 [*Erratum ibid.* **D 72** (2005) 119901] [`hep-ph/0509246`] [INSPIRE];
J.A. Cembranos, J.L. Feng and L.E. Strigari, *Exotic Collider Signals from the Complete Phase Diagram of Minimal Universal Extra Dimensions*, *Phys. Rev.* **D 75** (2007) 036004 [`hep-ph/0612157`] [INSPIRE];
S. Matsumoto, J. Sato, M. Senami and M. Yamanaka, *Productions of second Kaluza-Klein gauge bosons in the minimal universal extra dimension model at LHC*, *Phys. Rev.* **D 80** (2009) 056006 [`arXiv:0903.3255`] [INSPIRE];
G. Bhattacharyya, A. Datta, S.K. Majee and A. Raychaudhuri, *Exploring the Universal Extra Dimension at the LHC*, *Nucl. Phys.* **B 821** (2009) 48 [`arXiv:0904.0937`] [INSPIRE];

P. Bandyopadhyay, B. Bhattacherjee and A. Datta, *Search for Higgs bosons of the Universal Extra Dimensions at the Large Hadron Collider*, *JHEP* **03** (2010) 048 [`arXiv:0909.3108`] [ɪɴSPIRE];
B. Bhattacherjee and K. Ghosh, *Search for the minimal universal extra dimension model at the LHC with $\sqrt{s} = 7\,TeV$*, *Phys. Rev.* **D 83** (2011) 034003 [`arXiv:1006.3043`] [ɪɴSPIRE].

[8] H.-C. Cheng, J.L. Feng and K.T. Matchev, *Kaluza-Klein dark matter*, *Phys. Rev. Lett.* **89** (2002) 211301 [`hep-ph/0207125`] [ɪɴSPIRE].

[9] G. Servant and T.M.P. Tait, *Elastic scattering and direct detection of Kaluza-Klein dark matter*, *New J. Phys.* **4** (2002) 99 [`hep-ph/0209262`] [ɪɴSPIRE].

[10] E.A. Baltz and D. Hooper, *Kaluza-Klein dark matter, electrons and γ ray telescopes*, *JCAP* **07** (2005) 001 [`hep-ph/0411053`] [ɪɴSPIRE];
D. Hooper and J. Silk, *Searching for dark matter with future cosmic positron experiments*, *Phys. Rev.* **D 71** (2005) 083503 [`hep-ph/0409104`] [ɪɴSPIRE];
D. Hooper and G.D. Kribs, *Kaluza-Klein dark matter and the positron excess*, *Phys. Rev.* **D 70** (2004) 115004 [`hep-ph/0406026`] [ɪɴSPIRE].

[11] D. Hooper and G.D. Kribs, *Probing Kaluza-Klein dark matter with neutrino telescopes*, *Phys. Rev.* **D 67** (2003) 055003 [`hep-ph/0208261`] [ɪɴSPIRE];
A.E. Erkoca, M.H. Reno and I. Sarcevic, *Probing dark matter models with neutrinos from the Galactic center*, *Phys. Rev.* **D 82** (2010) 113006 [`arXiv:1009.2068`] [ɪɴSPIRE].

[12] A. Barrau et al., *Kaluza-Klein dark matter and Galactic antiprotons*, *Phys. Rev.* **D 72** (2005) 063507 [`astro-ph/0506389`] [ɪɴSPIRE];
T. Bringmann, *High-energetic cosmic antiprotons from Kaluza-Klein dark matter*, *JCAP* **08** (2005) 006 [`astro-ph/0506219`] [ɪɴSPIRE].

[13] G. Bertone, G. Servant and G. Sigl, *Indirect detection of Kaluza-Klein dark matter*, *Phys. Rev.* **D 68** (2003) 044008 [`hep-ph/0211342`] [ɪɴSPIRE]. L. Bergstrom, T. Bringmann, M. Eriksson and M. Gustafsson, *Gamma rays from Kaluza-Klein dark matter*, *Phys. Rev. Lett.* **94** (2005) 131301 [`astro-ph/0410359`] [ɪɴSPIRE].

[14] L. Bergstrom, T. Bringmann, M. Eriksson and M. Gustafsson, *Two photon annihilation of Kaluza-Klein dark matter*, *JCAP* **04** (2005) 004 [`hep-ph/0412001`] [ɪɴSPIRE].

[15] G.D. Mack, T.D. Jacques, J.F. Beacom, N.F. Bell and H. Yuksel, *Conservative Constraints on Dark Matter Annihilation into Gamma Rays*, *Phys. Rev.* **D 78** (2008) 063542 [`arXiv:0803.0157`] [ɪɴSPIRE].

[16] A. Abdo et al., *Fermi LAT Search for Photon Lines from 30 to 200 GeV and Dark Matter Implications*, *Phys. Rev. Lett.* **104** (2010) 091302 [`arXiv:1001.4836`] [ɪɴSPIRE].

[17] G. Bertone, C. Jackson, G. Shaughnessy, T.M.P. Tait and A. Vallinotto, *The WIMP Forest: Indirect Detection of a Chiral Square*, *Phys. Rev.* **D 80** (2009) 023512 [`arXiv:0904.1442`] [ɪɴSPIRE].

[18] L. Bergstrom and P. Ullio, *Full one loop calculation of neutralino annihilation into two photons*, *Nucl. Phys.* **B 504** (1997) 27 [`hep-ph/9706232`] [ɪɴSPIRE];
Z. Bern, P. Gondolo and M. Perelstein, *Neutralino annihilation into two photons*, *Phys. Lett.* **B 411** (1997) 86 [`hep-ph/9706538`] [ɪɴSPIRE];
P. Ullio and L. Bergstrom, *Neutralino annihilation into a photon and a Z boson*, *Phys. Rev.* **D 57** (1998) 1962 [`hep-ph/9707333`] [ɪɴSPIRE];
L. Bergstrom, P. Ullio and J.H. Buckley, *Observability of gamma-rays from dark matter neutralino annihilations in the Milky Way halo*, *Astropart. Phys.* **9** (1998) 137 [`astro-ph/9712318`] [ɪɴSPIRE];
F. Boudjema, A. Semenov and D. Temes, *Self-annihilation of the neutralino dark matter into two photons or a Z and a photon in the MSSM*, *Phys. Rev.* **D 72** (2005) 055024 [`hep-ph/0507127`] [ɪɴSPIRE].

[19] E. Dudas, Y. Mambrini, S. Pokorski and A. Romagnoni, *(In)visible Z-prime and dark matter*, *JHEP* **08** (2009) 014 [arXiv:0904.1745] [INSPIRE];
Y. Mambrini, *A Clear Dark Matter gamma ray line generated by the Green-Schwarz mechanism*, *JCAP* **12** (2009) 005 [arXiv:0907.2918] [INSPIRE];
C. Jackson, G. Servant, G. Shaughnessy, T.M.P. Tait and M. Taoso, *Higgs in Space!*, *JCAP* **04** (2010) 004 [arXiv:0912.0004] [INSPIRE];
C. Arina, T. Hambye, A. Ibarra and C. Weniger, *Intense Gamma-Ray Lines from Hidden Vector Dark Matter Decay*, *JCAP* **03** (2010) 024 [arXiv:0912.4496] [INSPIRE].

[20] M. Perelstein and A. Spray, *Indirect Detection of Little Higgs Dark Matter*, *Phys. Rev.* **D 75** (2007) 083519 [hep-ph/0610357] [INSPIRE];
M. Gustafsson, E. Lundstrom, L. Bergstrom and J. Edsjo, *Significant Gamma Lines from Inert Higgs Dark Matter*, *Phys. Rev. Lett.* **99** (2007) 041301 [astro-ph/0703512] [INSPIRE].

[21] J. Goodman, M. Ibe, A. Rajaraman, W. Shepherd, T.M.P. Tait and H.B.P. Yu, *Gamma Ray Line Constraints on Effective Theories of Dark Matter*, *Nucl. Phys.* **B 844** (2011) 55 [arXiv:1009.0008] [INSPIRE].

[22] H. Georgi, A.K. Grant and G. Hailu, *Brane couplings from bulk loops*, *Phys. Lett.* **B 506** (2001) 207 [hep-ph/0012379] [INSPIRE].

[23] H.-C. Cheng, K.T. Matchev and M. Schmaltz, *Radiative corrections to Kaluza-Klein masses*, *Phys. Rev.* **D 66** (2002) 036005 [hep-ph/0204342] [INSPIRE].

[24] M.S. Carena, T.M.P. Tait and C. Wagner, *Branes and orbifolds are opaque*, *Acta Phys. Polon.* **B 33** (2002) 2355 [hep-ph/0207056] [INSPIRE].

[25] T. Flacke, A. Menon and D.J. Phalen, *Non-minimal universal extra dimensions*, *Phys. Rev.* **D 79** (2009) 056009 [arXiv:0811.1598] [INSPIRE];
C. Csáki, J. Heinonen, J. Hubisz, S.C. Park and J. Shu, *5D UED: Flat and Flavorless*, *JHEP* **01** (2011) 089 [arXiv:1007.0025] [INSPIRE].

[26] G. Passarino and M. Veltman, *One Loop Corrections for e^+e^- Annihilation Into $\mu^+\mu^-$ in the Weinberg Model*, *Nucl. Phys.* **B 160** (1979) 151 [INSPIRE].

[27] R.G. Stuart, *Algebraic reduction of one loop Feynman diagrams to scalar integrals*, *Comput. Phys. Commun.* **48** (1988) 367 [INSPIRE].

[28] J.F. Navarro, C.S. Frenk and S.D. White, *The Structure of cold dark matter halos*, *Astrophys. J.* **462** (1996) 563 [astro-ph/9508025] [INSPIRE].

[29] J. Diemand, M. Zemp, B. Moore, J. Stadel and M. Carollo, *Cusps in CDM halos: The Density profile of a billion particle halo*, *Mon. Not. Roy. Astron. Soc.* **364** (2005) 665 [astro-ph/0504215] [INSPIRE].

[30] J.F. Navarro et al., *The Diversity and Similarity of Cold Dark Matter Halos*, arXiv:0810.1522 [INSPIRE].

[31] A.W. Graham, D. Merritt, B. Moore, J. Diemand and B. Terzic, *Empirical models for Dark Matter Halos. I. Nonparametric Construction of Density Profiles and Comparison with Parametric Models*, *Astron. J.* **132** (2006) 2685 [astro-ph/0509417] [INSPIRE].

[32] G.R. Blumenthal, S. Faber, R. Flores and J.R. Primack, *Contraction of Dark Matter Galactic Halos Due to Baryonic Infall*, *Astrophys. J.* **301** (1986) 27 [INSPIRE].

[33] J. Edsjo, M. Schelke and P. Ullio, *Direct versus indirect detection in mSUGRA with self-consistent halo models*, *JCAP* **09** (2004) 004 [astro-ph/0405414] [INSPIRE].

[34] F. Prada, A. Klypin, J. Flix Molina, M. Martinez and E. Simonneau, *Dark Matter Annihilation in the Milky Way Galaxy: Effects of Baryonic Compression*, *Phys. Rev. Lett.* **93** (2004) 241301 [astro-ph/0401512] [INSPIRE].

[35] O.Y. Gnedin, A.V. Kravtsov, A.A. Klypin and D. Nagai, *Response of dark matter halos to condensation of baryons: Cosmological simulations and improved adiabatic contraction model*, *Astrophys. J.* **616** (2004) 16 [`astro-ph/0406247`] [ɪɴSPIRE].

[36] G. Bertone and D. Merritt, *Time-dependent models for dark matter at the Galactic Center*, *Phys. Rev.* **D 72** (2005) 103502 [`astro-ph/0501555`] [ɪɴSPIRE].

[37] O. Agertz, R. Teyssier and B. Moore, *The formation of disk galaxies in a LCDM universe*, `arXiv:1004.0005` [ɪɴSPIRE].

[38] F. Bigiel et al., *The Star Formation Law in Nearby Galaxies on Sub-Kpc Scales*, *Astron. J.* **136** (2008) 2846 [`arXiv:0810.2541`] [ɪɴSPIRE].

[39] M. Pato, O. Agertz, G. Bertone, B. Moore and R. Teyssier, *Systematic uncertainties in the determination of the local dark matter density*, *Phys. Rev.* **D 82** (2010) 023531 [`arXiv:1006.1322`] [ɪɴSPIRE].

[40] P. Gondolo and J. Silk, *Dark matter annihilation at the galactic center*, *Phys. Rev. Lett.* **83** (1999) 1719 [`astro-ph/9906391`] [ɪɴSPIRE].

[41] D. Merritt, M. Milosavljevic, L. Verde and R. Jimenez, *Dark matter spikes and annihilation radiation from the galactic center*, *Phys. Rev. Lett.* **88** (2002) 191301 [`astro-ph/0201376`] [ɪɴSPIRE].

[42] P. Ullio, H. Zhao and M. Kamionkowski, *A Dark matter spike at the galactic center?*, *Phys. Rev.* **D 64** (2001) 043504 [`astro-ph/0101481`] [ɪɴSPIRE].

[43] E.W. Kolb, G. Servant and T.M.P. Tait, *The Radionactive universe*, *JCAP* **07** (2003) 008 [`hep-ph/0306159`] [ɪɴSPIRE];
K. Chan and M.-C. Chu, *Cosmological Constraints on Radion Evolution in the Universal Extra Dimension Model*, *Phys. Rev.* **D 77** (2008) 063525 [`arXiv:0708.0122`] [ɪɴSPIRE].

[44] N.R. Shah and C.E. Wagner, *Gravitons and dark matter in universal extra dimensions*, *Phys. Rev.* **D 74** (2006) 104008 [`hep-ph/0608140`] [ɪɴSPIRE].

[45] V. Vitale, A. Morselli and ꜰ.ᴛ.ꜰ. collaboration, *Indirect Search for Dark Matter from the center of the Milky Way with the Fermi-Large Area Telescope*, `arXiv:0912.3828` [ɪɴSPIRE].

[46] H.E.S.S. collaboration, F. Aharonian, *Spectrum and variability of the Galactic Center VHE gamma-ray source HESS J1745-290*, *Astron. Astrophys.* **503** (2009) 817 [`arXiv:0906.1247`] [ɪɴSPIRE].